SPECTROSCOPIC, STRUCTURAL AND THERMAL CHARACTERIZATION OF CRYSTALLINE [Cr(OC(NH$_2$)$_2$)$_6$]X$_3$ (X = ClO$_4$, BF$_4$ AND Cl) COMPLEXES

Natalia Górska,[a] Edward Mikuli[a] and László Kótai[b]

Three coordination compounds with urea (CO(NH$_2$)$_2$) ligands, namely [Cr(urea)$_6$](ClO$_4$)$_3$, [Cr(urea)$_6$](BF$_4$)$_3$, and [Cr(urea)$_6$]Cl$_3$ were investigated. In the temperature range of 130–320 K only the first two aforementioned complexes undergo one solid phase transition at: T^h_C =298.4 K and T^h_C=255.4 K (on heating), respectively. X-ray single crystal diffraction at 293 K demonstrates that [Cr(urea)$_6$](BF$_4$)$_3$ crystallises in the trigonal crystal system (*R*-3*c* space group) and is isostructural with the other two title compounds. Both the BF$_4^-$ anions and CO(NH$_2$)$_2$ ligands are in the high temperature phase dynamically disordered. [Cr(urea)$_6$](ClO$_4$)$_3$, [Cr(urea)$_6$](BF$_4$)$_3$ and [Cr(urea)$_6$]Cl$_3$ are thermally stable up to ca. 500, 470 and 440 K, respectively, in argon atmosphere. [Cr(urea)$_6$](ClO$_4$)$_3$ decomposes explosively at ca. 550 K. [Cr(urea)$_6$](BF$_4$)$_3$ decomposes in three main stages with creation of Cr$_2$O$_3$ as a final product of decomposition at 1250 K. Whereas [Cr(urea)$_6$]Cl$_3$ decomposes in two main stages. The mixture of Cr, CrCl$_3$ and ClCrNH is created at 1270 K as a product of decomposition.

Corresponding Authors
    Tel: +48 12 663 2265
    E-Mail: gorska@chemia.uj.edu.pl
[a]   Faculty of Chemistry, Jagiellonian University, Ingardena 3, 30-060 Kraków, Poland,
[b]   Institute of Chemistry, Chemical Research Center, Hungarian Academy of Sciences, H-1525 Budapest, P.O. Box 17, Hungary

Introduction

It has been proved that metal-urea complexes are useful precursors to synthesize various nanocrystalline materials like metal oxides or nitrides.[1-3] [Ti(urea)$_6$]Cl$_3$ is a molecular precursor for nanocrystalline TiO$_2$ via thermal decomposition.[1] This complex is formed via C=O····Ti bonding and crystallizes in hexagonal space group *P*-3*c*1. It decomposes under stagnant air atmosphere in three main steps between 500 and 720 K. The final product of this decomposition, after oxidation of Ti^{3+} to Ti^{4+}, is crystalline TiO$_2$. In turn, [Al(urea)$_6$]Cl$_3$ decomposes under argon atmosphere in three main steps and the final decomposition product above 920 K is (ClAlNH)$_n$, which can be converted to nanocrystalline *c*- and *h*-AlN under NH$_3$ atmosphere.[2]

Crystal structure and thermal behaviour of six-coordinate compounds of the [M(urea)$_6$]X$_3$ type, with M = Mn^{3+}, Al^{3+}, Ti^{3+}, V^{3+} and X = ClO$_4^-$, ClO$_3^-$, NO$_3^-$, Cl$^-$, I$^-$, have been already investigated.[4-15] [Mn(urea)$_6$](ClO$_4$)$_3$ undergoes one phase transition between 290 and 317 K detected by different scanning calorimetry (DSC) method.[9] A second order phase transition has been also observed in [Al(urea)$_6$](ClO$_4$)$_3$ at ca. 295 K and in [Ga(urea)$_6$](ClO$_4$)$_3$ at ca. 301 K, by Mooy et al. using electron spin resonance (ESR) method.[10-12] These transitions are of the second order and antiferro-distortive and of displacive type. In the model proposed the phase transition was triggered by ordering of the oxygen atoms orientation in the perchlorate ions, half of which are assumed to be disordered above T_C.

The compounds of the [M(urea)$_6$](ClO$_4$)$_3$ type with M=Mn^{3+}, Al^{3+}, Ti^{3+} and V^{3+} are isomorphous at room temperature and crystallize in the hexagonal space group *R*-3*c* with *Z*=6.[11,13-15] In all mentioned compounds the perchlorate anions of tetrahedral symmetry are disordered. The structure consists of a two-dimensional close-packed arrangement of trigonally distorted octahedral [M(urea)$_6$]$^{3+}$ units in columns parallel to the *c* axis. In the columnar interstices the perchlorate ions are arranged in spiral fashion. The structure is loosely linked by hydrogen bonding net and van der Waals contacts.

The crystal structure of [Ti(urea)$_6$](ClO$_4$)$_3$ was also investigated at 90 K.[15] At this temperature it crystallizes in the same space group *R*-3*c*. The lattice parameter *c* is slightly smaller than the high-temperature value, but the parameter *a* is nearly twice as large as the one observed in high-temperature phase. The doubling value of parameter *a* is attributed to freezing out of the perchlorate ions below the phase transition temperature. So far, there is no information in literature about phase behaviour of the [M(urea)$_6$](BF$_4$)$_3$ compounds.

Among six coordination metal(III) complexes with ClO$_4^-$ and BF$_4^-$ tetrahedral anions, the phase polymorphism of [M(NH$_3$)$_6$](ClO$_4$)$_3$,[16-18] [M(NH$_3$)$_6$](BF$_4$)$_3$,[19-21] [M(H$_2$O)$_6$](ClO$_4$)$_2$,[22-23] and [M(DMSO)$_6$](ClO$_4$)$_2$[24-25] has been thoroughly investigated.

The main subject of the present paper is spectroscopic, structural and thermal characterization and investigation of phase polymorphism of three [Cr(OC(NH$_2$)$_2$)$_6$]X$_3$ ionic compounds, with ClO$_4^-$, BF$_4^-$, and Cl$^-$ anions, using vibrational (FT-IR and FT-Raman) and electronic (UV-Vis) spectroscopies, X-ray single crystal diffraction (XRSCD), differential scanning calorimetry (DSC), and thermogravimetry analysis (TG/QMS).

Experimental

Materials and methods

Synthetic procedures. [Cr(urea)$_6$]Cl$_3$ (hereafter referred to as CrUCl) was prepared according to the method proposed by A. Werner.[26] [Cr(urea)$_6$](ClO$_4$)$_3$ (CrUClO) and [Cr(urea)$_6$](BF$_4$)$_3$ (CrUBF) were synthesized at room temperature by dissolving 1 gram of [Cr(urea)$_6$]Cl$_3$ in 20 ml of double distilled water and then stoichiometric amounts of aqueous solution of NH$_4$ClO$_4$ (99% purity, Sigma Aldrich) or NaBF$_4$ (99% purity, Sigma Aldrich), respectively, were added. The green precipitates formed as very fine needles were washed with distilled water and dried in air at 60 °C in order to remove water. They were stored in sealed containers in a desiccator over P$_4$O$_{10}$. The contents of carbon, nitrogen and hydrogen of the OC(NH$_2$)$_2$ (urea) ligands in the compounds investigated were determined from elemental analysis using a CHNS Vario Micro Cube instrument with a TCD detector. Calculated % for CrUCl: C, 13.89, N, 32.40; H, 4.66. Found %: C, 13.69, N, 32.23; H, 4.60. Calculated % for CrUClO: C, 10.14, N, 23.65; H, 3.40. Found %: C, 10.11, N, 23.46; H, 3.42. Calculated % for CrUBF: C, 10.71, N, 24.98; H, 3.60. Found %: C, 10.61, N, 24.89; H, 3.50. The presence of six urea ligands in the [Cr(urea)$_6$]$^{3+}$ cation unit of all three compounds investigated in the examined samples was confirmed.

FT-IR. Fourier transform middle infrared absorption (FT-MIR) spectra (4000–500 cm^{-1}) were performed using a Bruker VERTEX 70v vacuum spectrometer. The globar as a light source and a DTGS detector were used. The spectra were collected with a resolution of 2 cm^{-1} and 32 scans per each spectrum. The powdered samples were suspended in KBr pellets. Fourier transform far infrared absorption (FT-FIR) spectra (500–100 cm^{-1}) were collected for samples suspended in Apiezon N grease and placed on a polyethylene (PE) disc. The spectra were collected with a resolution of 2 cm^{-1} and 64 scans per spectrum.

FT-RS. Fourier transform Raman light scattering spectra were obtained with a Multi-RAM FT-Raman Bruker spectrometer at a frequency range 4000–50 cm^{-1}, with a resolution of 4 cm^{-1} and with 256 scans accumulated per each spectrum. A YAG Spectra-Physics Neodymium laser was used with incident radiation λ = 1064 nm.

UV-VIS. A Shimadzu UV–2101PC spectrophotometer equipped with ISR-260 attachment was used to record the electronic reflectance spectra in BaSO$_4$ pellets with BaSO$_4$ as a reference. The spectra were recalculated to absorbance units using the Kubelka–Munk transformation.

XRSCD. X-ray single crystal diffraction measurement was performed at 293 K for [Cr(urea)$_6$](BF$_4$)$_3$ using an Oxford Diffraction SuperNova four-circle diffractometer. Needle shaped green crystal of good quality was investigated. Crystallographic data have been deposited at the CCDC, 12 Union Road, Cambridge CB2 1EZ, UK. The deposition number is 995339.

DSC. Differential scanning calorimetry (DSC) measurements were conducted between 130 and 400 K using a Mettler-Toledo 822^e instrument. Powdered samples of [Cr(urea)$_6$](ClO$_4$)$_3$, [Cr(urea)$_6$](BF$_4$)$_3$, and [Cr(urea)$_6$]Cl$_3$

with masses of 8.45, 5.65, and 5.88 mg, respectively, were placed in hermetically sealed aluminium pans and measured with a scanning rate of 20 K min^{-1}. The transition temperatures were considered to be the peak temperature (T_{peak}) from the DSC curves on heating and cooling. Additional DSC measurement was conducted during heating for the [Cr(urea)$_6$](ClO$_4$)$_3$ sample placed in hermetically sealed aluminium pan with a hole on top with a scanning rate of 10 K min^{-1} in temperatures between 135 and 570 K. The sample mass was 2.63 mg. Additional DSC measurements were performed at 93–297 K with a Perkin Elmer PYRIS 1 DSC apparatus. The instrument was calibrated using the literature data for indium and water melting points. The enthalpy change (∆H) was calculated by numerical integration of the DSC curve under the anomaly peak after a linear background arbitrary subtraction. The entropy change (∆S) was calculated using the formula: ∆S =∆H/T_C. The powdered samples were placed in aluminium vessels and closed by compression. The measurements were made both on heating and on cooling a freshly synthesized samples of [Cr(urea)$_6$](ClO$_4$)$_3$ and [Cr(urea)$_6$](BF$_4$)$_3$ of masses equal to 9.37 and 7.60 mg, respectively, with constant scanning rate of 20 K min^{-1}.

TGA. To characterize the samples further, thermal analysis was performed using thermogravimetry with simultaneous differential thermal analysis (TGA/DTG/SDTA) by means of a Mettler-Toledo TGA/SDTA 851e instrument. The gaseous products evolved from decomposition were identified on an on-line quadruple mass spectrometer (QMS) using a Balzer GSD 300T instrument. Powdered samples of [Cr(urea)$_6$](ClO$_4$)$_3$, [Cr(urea)$_6$](BF$_4$)$_3$, and [Cr(urea)$_6$]Cl$_3$ with masses of 3.719, 9.157, and 11.071 mg, respectively, were placed in open corundum crucible and measured with a scanning rate of 10 K min^{-1}. The measurements were performed at 300–1270 K with a constant flow (80 mL min^{-1}) of dry argon (99.999 %).

Results and discussion

Vibrational spectra (FT-IR and FT-RS)

The complex cation [Cr(urea)$_6$]$^{3+}$ is expected to have octahedral symmetry with the OC(NH$_2$)$_2$ ligands being coordinated to the central cation Cr^{3+} through oxygen atoms. The FT-IR and FT-RS band positions, their relative intensities and their tentative assignments are listed in Table 1. Comparison of the IR and Raman spectra of all three compounds are summarized in Fig. 1.

The proper assignment of the bands observed in FT-IR and FT-RS spectra of the chromium(III) compounds studied was done by comparison with the spectra obtained for pure urea and similar hexakis(urea-O)metal(III) coordination compounds published earlier.[1,2,27–29] Clearly, the strong C=O stretching vibration observed for free urea molecule at 1684 cm^{-1}, strongly coupled with δ_s(NH$_2$) mode, is shifted toward lower frequency in the case of urea molecules octahedrally coordinated to central metal through oxygen atoms. In turn, the C-N stretching vibration observed for free urea at 1466 cm^{-1} shifts toward higher frequency in case of all three compounds studied. Overall, the assignment proved that the molecular structures of the investigated compounds are such as expected.

Table 1. List of band positions of FT-IR and FT-Raman spectra of $[Cr(urea)_6]X_3$, where X = ClO_4^-, BF_4^-, and Cl^- with tentative assignments.

FT-IR, cm⁻¹			FT-Raman, cm⁻¹			Tentative assignments
ClO_4^- in 310 K	BF_4^- in 293 K	Cl^- in 293 K	ClO_4^- in 293 K	BF_4^- in 293 K	Cl^- in 293 K	
3491 st	3504 st	3451 vst	3485 w	3503 w	3442 sh	$\nu_{as}(NH_2)$
3477 sh			3479 w	3411 m		$\nu_{as}(NH_2)$
3374 st	3392 st	3352 vst	3397 m	3386 sh	3340 m	$\nu_s(NH_2)$
			3371 sh		3267 sh	$\nu_s(NH_2)$
3252 w	3261 w	3202 vst			3208 m	$\delta_s(NH_2)+\nu(CO)$
3199 w	3203 w					$\delta_s(NH_2)+\nu(CO)$
3133 w	3142 w					$\delta_s(NH_2)+\nu(CO)$
		2794 br,m				
1662 sh	1670 sh	1634 vst		1651 w,sh	1690 vw	$\delta_s(NH_2)$
1632 vst	1635 st		1630 w	1633 w	1647 w	$\delta_{as}(NH_2)$
					1618 w	$\delta_{as}(NH_2)/\nu(CO)$
1554 st	1557 st	1568 st	1566 w	1570 m	1580 sh	$\nu(CO)$
1545 sh	1548 sh	1553 sh	1557 m	1560 w,sh	1564 m	$\nu(CO)+\delta(NH_2)$
1510 m	1513 m	1499 st	1505 m	1507 m	1499 m	$\nu_{as}(CN)$
1500 sh		1466 st				
		1402				
	1296 w					
1150 sh	1155 sh	1161 sh	1144 vw	1150 w	1176 w	$\rho(NH_2)$
1091 st			1105 w			$\nu_{as}(ClO)F_2$
1036 sh	1043 vst	1034 sh	1042 st	1042 st	1040 st	$\nu_s(CN)$
	1029 vst,sh			1005 w,sh		$\nu_{as}(BF)F_2$
942 w,sh			938 vst			$\nu_s(ClO)A_1$
910 w,sh			911 sh			
825 vw,br			826 vw			
770 w	771 vw	764 m	774 w	784 vw		$\omega(CO)$
				770 vst		$\nu_s(BF)A_1$
758 w	758 w		760 w	758 vw	765 vw	$\tau_{as}(NH_2)$
	685w					
635 sh	631 st	634 m	629 st	628 st	631 st	
626 st			606 w,sh			$\delta_{as}(ClO)F_2$
	579 w	560 m				$\delta(CO)$
544 st	543 st	546 m	546 w	546 m	557 st	$\delta(CN)$
537 st		538 m	531 w		535 m	
	530 sh			530 m		$\delta_{as}(BF)F_2$
504	502 w					$\omega_a(NH_2)$
			465 st			$\delta_s(ClO)E$
450 w,br	425 m,br	462 m,br	458 st,sh			$\nu(M-O)$
377 st	371 st	389 st				
	349 sh			355 w		$\delta_s(BF)E$
311 w			309 w	308 w	312 w	
		252 w	273 vw	273 vw	280 vw	(O-Cr-O)
224 m	224 m	230 w	217 w			(O-Cr-O)
	216 sh	195 w		202 w	203 m	
	200 m					
198 m	192 m					
	185 w					
144 m	147 w	166 w	158 sh		167 m	Lattice
			114 vst	115 vst	103 vst	Lattice
			76 m,sh	73 m,sh	81 vst	Lattice

(vw – very weak, w – weak, sh – shoulder, m – medium, st – strong, vst – very strong, br – broad, ρ – rocking, τ – torsional, ω – wagging).
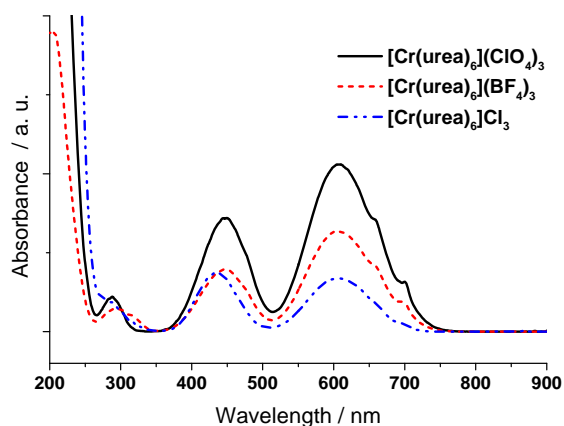
Electronic spectra (UV-Vis)

For further verification of the composition of the title compounds the UV-Vis spectra were measured. The results are presented in Fig. 2.

The electronic spectra of all three hexakis(urea-O)chromium(III) compounds, which have octahedral symmetry, are very similar and are essentially independent of the anion in the lattice. According to crystal field theory for the d^3 electronic configuration in octahedral ligand environment
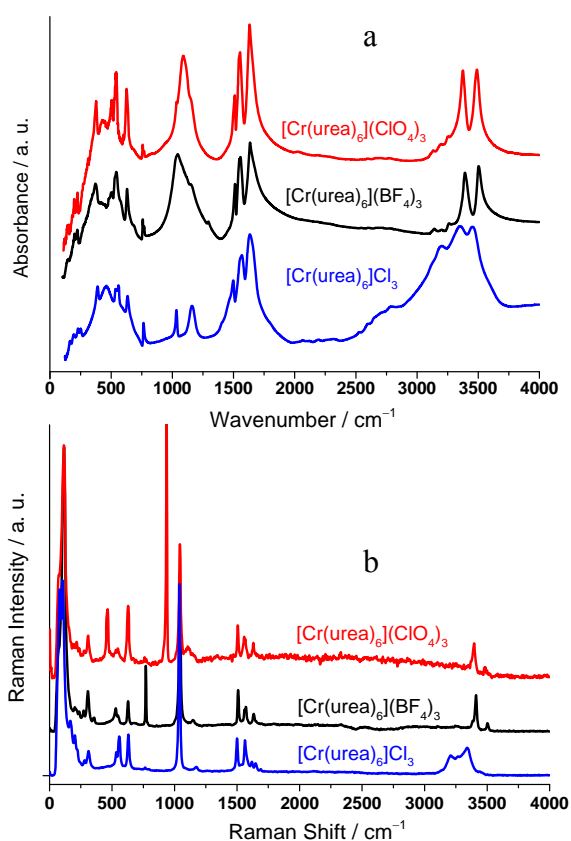
Figure 1. Comparison of experimental FT-IR (a) and FT-Raman (b) spectra of all three compounds investigated.

the lowest energy state for investigated compounds is designated to $^4A_{2g}$, thus exhibit three spin-allowed transitions from the ground state $^4A_{2g}$ to the excited states: $^4T_{2g}(F)$, $^4T_{1g}(F)$ and $^4T_{1g}(P)$, in order of increasing energy.[30-32] In the spectrum of $[Cr(urea)_6](ClO_4)_3$ there are indeed three main bands observed at: 608, 446, and 288 nm, which are attributed to $^4A_{2g} \rightarrow {}^4T_{2g}(F)$, $^4A_{2g} \rightarrow {}^4T_{1g}(F)$ and $^4A_{2g} \rightarrow {}^4T_{1g}(P)$ transitions, respectively. The band positions of the other two compounds investigated, namely $[Cr(urea)_6](BF_4)_3$ and $[Cr(urea)_6]Cl_3$, appear almost at the same wavelengths. The bands positions observed in the electronic spectra together with their assignments are presented in Table 2. The electronic spectra (Fig. 2) additionally confirm the proper composition of the title complexes.

Figure 2. Electronic spectra obtained at room temperature for all three compounds investigated.

Table 2. Wavelengths and frequencies (nm/cm⁻¹) of the observed d-d transitions in Cr-urea complexes.

| [Cr(urea)₆]X₃	$^4A_{2g} \rightarrow {}^4T_{2g}(F)$	$^4A_{2g} \rightarrow {}^4T_{1g}(F)$	$^4A_{2g} \rightarrow {}^4T_{1g}(P)$
Perchlorate	608/16447	446/22422	288/34722
Tetrafluoroborate	605/16529	448/22321	294/34014
Chloride	607/16474	434/23041	~273/36630

Crystal structure of [Cr(urea)₆](BF₄)₃ at 293 K

In order to check if $[Cr(urea)_6](BF_4)_3$ coordination compound is isostructural to $[Cr(urea)_6](ClO_4)_3$ and $[Cr(urea)_6]Cl_3$ investigated earlier[32] the X-ray single crystal diffraction measurement was performed. Table 3 presents experimental details of this experiment at 293 K.

Table 3. Crystallographic data for [Cr(urea)₆](BF₄)₃ at 293 K.

CCDC	995339
Crystallographic method	Single-crystal diffraction
Radiation	μ(MoKα) (λ = 0.71073 Å)
Empirical formula	$C_6H_{24}B_3F_{12}N_{12}O_6Cr$
Formula weight	672.80 g mol⁻¹
Crystal size	0.500 x 0.100 x 0.050 mm³
Temperature	293(2) K
Crystal system	Trigonal
Space group	R-3c (No. 167)
Unit cell dimensions	a = 17.8250(5) Å
	b = 17.8250(5) Å
	c = 13.9010(8) Å
	α, γ = 90°, β = 120°
Volume	3825.0(3) Å³
D_{calc}	1.752 g cm⁻¹
Z	6
F_{000}	2034
Θ range for data collect.	2.28 to 27.62°
Reflections collected	8903
Independent reflections	989 (R_{int}=0.0416)
Refinement method	Full-matrix least-squares on F^2
Data/restrains/parameters	989/4/89
Goodness of Fit on F^2	1.208
Final R indices [I> 2sigma(I)]	R_1 = 0.0471, wR_2 = 0.1317
R indices (all data)	R_1 = 0.0608, wR_2 = 0.1578

The $[Cr(urea)_6](BF_4)_3$ compound studied crystallizes in the trigonal space group R-3c with lattice parameters a = b = 17.8250(5) Å, c = 13.9010(8) Å, and α, γ = 90°, β = 120°, and Z = 6. Figure 3 presents a grow fragment in the unit cell and the molecular packing viewed along the c axis of $[Cr(urea)_6](BF_4)_3$. Each Cr^{3+} cation is coordinated by six urea molecules through oxygen atoms with all the Cr–O distances equivalent and equal to 1.963 Å and with the O–Cr–O bond angles ranging from 92.72 to 85.56°. All BF_4^- anions exhibit dynamical disorder at this temperature. Detailed geometrical parameters with atomic coordinates and isotropic displacement parameters are listed in Table 4 and selected bond lengths and angles are compared in Table 5.

Eur. Chem. Bull., **2014**, *3(5),* 474-481

477
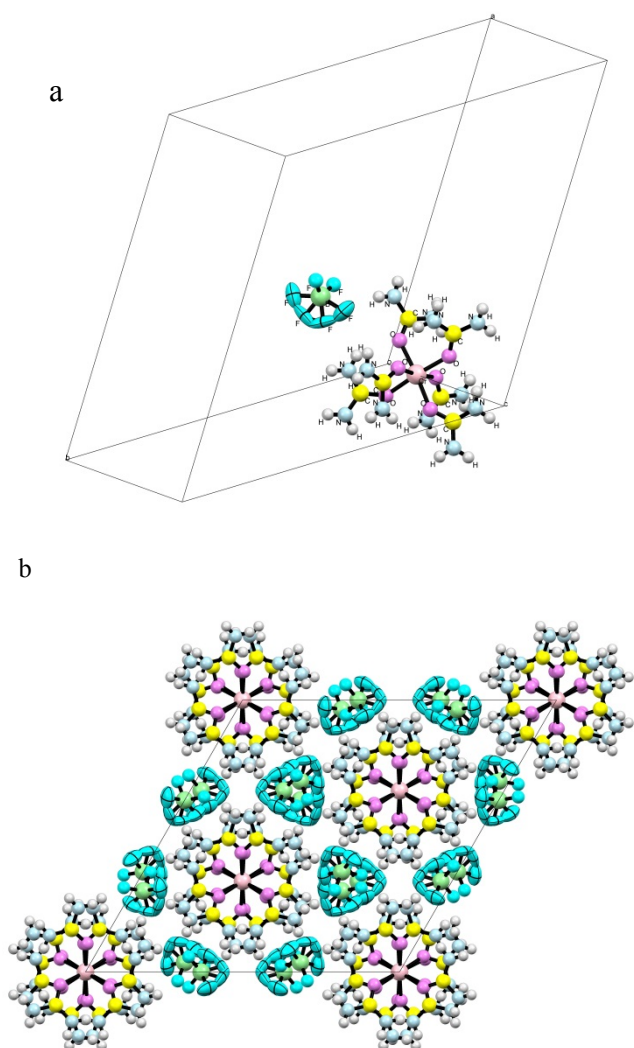
Figure 3. A view of (a) a grow fragment and (b) molecular packing of the unit cell along *c* axis of [Cr(urea)₆](BF₄)₃ at 293 K.

Phase transition investigations

Two temperature dependences of the heat flow (two DSC curves) of the [Cr(urea)₆](ClO₄)₃ and [Cr(urea)₆](BF₄)₃ samples registered during cooling (lower curves) and subsequent heating (upper curves) with a scanning rate of 20 K min⁻¹ are presented in Fig. 4.
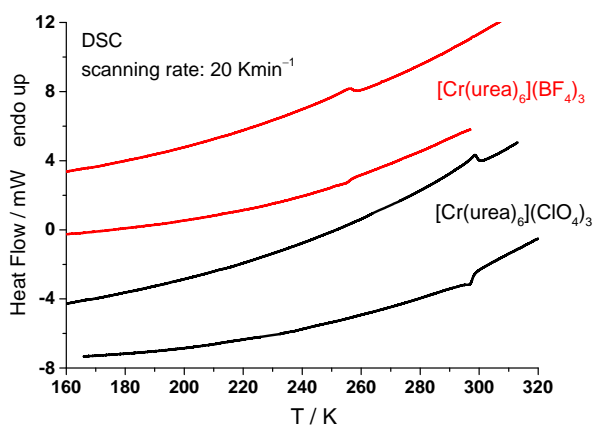
Figure 4. DSC curves for [Cr(urea)₆](BF₄)₃ and [Cr(urea)₆](ClO₄)₃ registered on cooling (lower curves) and heating (upper curves) with a scanning rate of 20 K min⁻¹.

Table 4. Atomic coordinates and equivalent isotropic displacement parameters U_{eq}/ $(10^3$ Å^2) for the structure obtained for [Cr(OC(NH₂)₂)₆](BF₄)₃ at 293 K.

Atom	x	y	z	U(eq)
Cr(1)	0.0000	0.0000	0.2500	0.033(1)
O(1)	0.1045(1)	0.0571(1)	0.1699(1)	0.042(1)
N(3)	0.1345(2)	-.0476(2)	0.1296(2)	0.062(1)
N(4)	0.2348(2)	0.0945(2)	0.1109(2)	0.061(1)
C(2)	0.1561(2)	0.0339(2)	0.1368(2)	0.042(1)
F(11)	0.3101(2)	0.2772(2)	0.0298(2)	0.091(1)
F(12A)	0.2224(4)	0.3121(1)	0.1144(12)	0.119(9)
F(12B)	0.2489(9)	0.2740(5)	0.1619(7)	0.114(5)
B(1)	0.2981(3)	0.3333	0.0833	0.055(1)
H(3A)	0.086(2)	-0.090(2)	0.142(3)	0.068(12)
H(4A)	0.249(2)	0.1468(14)	0.112(3)	0.061(10)
H(3B)	0.173(2)	-0.059(2)	0.111(3)	0.069(10)
H(4B)	0.271(2)	0.084(2)	0.081(3)	0.070(11)

U_{eq} is defined as one third of the trace of the orthogonalized U^{ij} tensor.

Table 5. Selected interatomic distances (Å) and angles (°) in [Cr(urea)₆](BF₄)₃ determined from XRSCD at 293 K.

Bond	Distances (Å)
Cr(1)–O(1)	1.9630(17)
O(1)–C(2)	1.268(3)
N(3)–C(2)	1.307(3)
N(4)–C(2)	1.323(4)
F(11)–B(1)	1.347(3)
F(12A)–B(1)	1.280(7)
F(12B)–B(1)	1.467(7)
N(3)–H(3A)	0.830(18)
N(3)–H(3B)	0.846(19)
N(4)–H(4A)	0.835(19)
N(4)–H(4B)	0.864(19)

Bond	Angles (°)
O(1)–Cr(1)–O(1)#1	85.56(10)
O(1)–Cr(1)–O(1)#2	90.97(8)
O(1)#1–Cr(1)–O(1)#2	174.97(9)
O(1)–Cr(1)–O(1)#3	90.97(8)
O(1)#1–Cr(1)–O(1)#3	92.72(10)
C(2)–O(1)–Cr(1)	133.74(17)
C(2)–N(3)–H(3A)	125(3)
C(2)–N(3)–H(3B)	118(3)
C(2)–N(4)–H(4A)	121(3)
C(2)–N(4)–H(4B)	124(2)
O(1)–C(2)–N(3)	122.2(2)
O(1)–C(2)–N(4)	118.5(3)
N(3)–C(2)–N(4)	119.3(3)
F(11)–B(1)–F(11)	116.0(4)
F(12A)–B(1)–F(12B)	51.3(5)

One small and broad anomaly at T^h_C=298.4 K (on heating) and T^c_C=296.7 K at (on cooling) can be observed for [Cr(urea)₆](ClO₄)₃. Also, one small and broad anomaly can be observed for [Cr(urea)₆](BF₄)₃, but it is shifted almost 40 K to lower temperature, namely: T^h_C=255.4 K (on heating)

and $T^c{}_C$=254.5 K at (on cooling). Thus, both compounds exhibit one solid-solid phase transition. We did not observe any phase transition in [Cr(urea)₆]Cl₃ in the temperature range investigated. The thermodynamic parameters of these transitions are shown in Table 6. Small thermal hysteresis (less than 2 degree) suggest that both phase transitions are rather of order-disorder type and are not connected with a large structural change.

Table 6. Thermodynamic parameters of the phase transition observed in [Cr(urea)₆](ClO₄)₃ and [Cr(urea)₆](BF₄)₃, obtained with a scanning rate of 20 K min⁻¹.

	T_C, K	ΔH, J mol⁻¹	ΔS, J K⁻¹ mol⁻¹
[Cr(urea)₆](ClO₄)₃			
Heating	298.4	1784	6.0
Cooling	296.7	2009	6.8
[Cr(urea)₆](BF₄)₃			
Heating	255.4	1630	6.4
Cooling	254.5	1460	5.7

Interestingly, the observed phase transition in [Cr(urea)₆](ClO₄)₃ occurs at very similar temperature ($T^h{}_C$=298.4 K) to the ones observed in [Ru(NH₃)₆](ClO₄)₃ ($T^h{}_C$=290.3 K) detected by adiabatic calorimetry[17] and [Cr(NH₃)₆](ClO₄)₃ ($T^h{}_C$=293.5 K) detected by DSC.[18] In turn, the transition in [Cr(urea)₆](BF₄)₃ occurs at similar temperature ($T^h{}_C$=255.4 K) to the ones observed in [Ru(NH₃)₆](BF₄)₃ ($T^h{}_C$=241.6 K)[19], [Co(NH₃)₆](BF₄)₃ ($T^h{}_C$=271.7 K)[20], and [Cr(DMSO)₆](BF₄)₃ ($T^h{}_C$=247.4 K)[33], all of them detected by adiabatic calorimetry. It confirms an important role of the anion in phase transition mechanism.

Thermal stability (TG/ DTG/QMS)

DSC curve obtained during heating of the [Cr(urea)₆](ClO₄)₃ sample is presented in Fig. 5. The sample is stable up to about 500 K. Above this temperature large exothermic upturn above 550 can be observed which is a result of explosive decomposition. About the same temperature of decomposition was obtained by us for the sample measured in an open corundum crucible (without a lid). The inset to Fig. 5 shows a magnified view of heat flow between 250 K and 340 K. A small endothermic peak can be observed at about 300 K, which is associated with the solid-solid phase transition previously described.

The TG, DTG and QMS curves for [Cr(urea)₆](BF₄)₃ are presented in Fig.6. The masses of m/e = 43, 17, 16, 28, 44, 18, 27, 30, 26, 48, 19, and 46 correspond to fragments of HNCO, NH₃ or OH, O or NH₂, N₂, BNF or CO₂ or N₂O, H₂O, HCN, NO or BF, CN, BF₂, F, and NO₂, respectively. The thermal decomposition of the sample proceeds in three main stages. The sample is thermally stable up to about 470 K. Above this temperature in the range of 470–510 K it decomposes liberating two urea ligands. 83.6 % of the initial mass of the sample remains at 510 K, and this value corresponds well to the theoretical amount (82.2 %) of tetrakis(urea)chromium(III) tetrafluoroborate. In the second stage in the range of 510–655 K, most probably the next four urea molecules are liberated and the decomposition products of urea react with chromium(III) tetrafluoroborate creating an intermediate adducts.
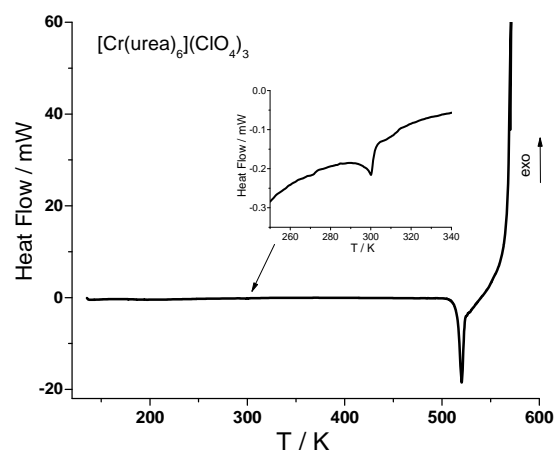

Figure 5. DSC curve for [Cr(urea)₆](ClO₄)₃ registered on heating with a constant rate of 10 K min⁻¹.

Both processes occur simultaneously but the exact mechanism of the second stage of decomposition is difficult to identify. In the third stage in the range of 655–1250 K, the intermediate adduct decomposes with further liberating of N₂, NO₂, F, CN, and HCN among others (see QMS lines in Fig. 6). The final product of thermal decomposition of [Cr(urea)₆](BF₄)₃ at 1250 K is chromium(III) oxide (Cr₂O₃) what was confirmed by us with FT-IR spectroscopy.
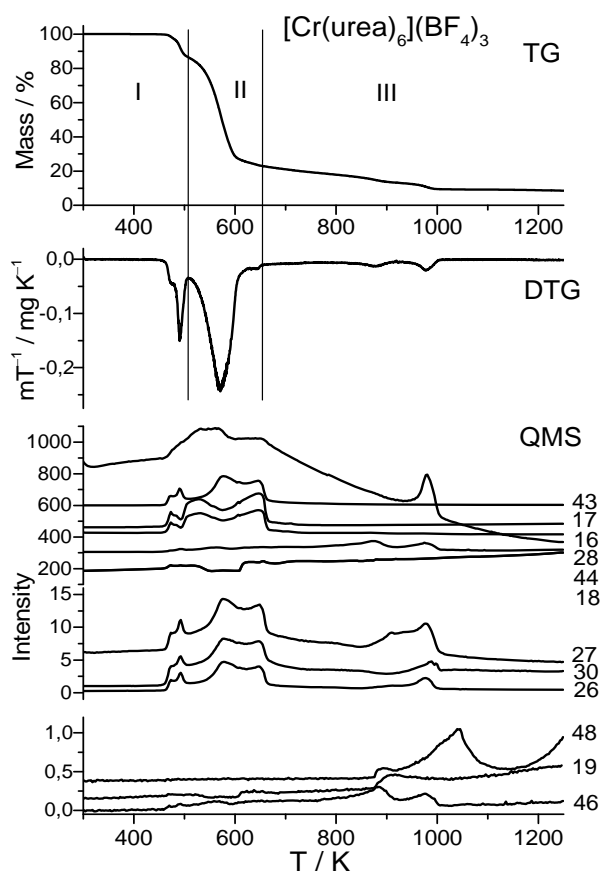
Figure 6. TG, DTG, and QMS curves obtained for [Cr(urea)₆](BF₄)₃ during heating with a constant rate of 10 K min⁻¹.
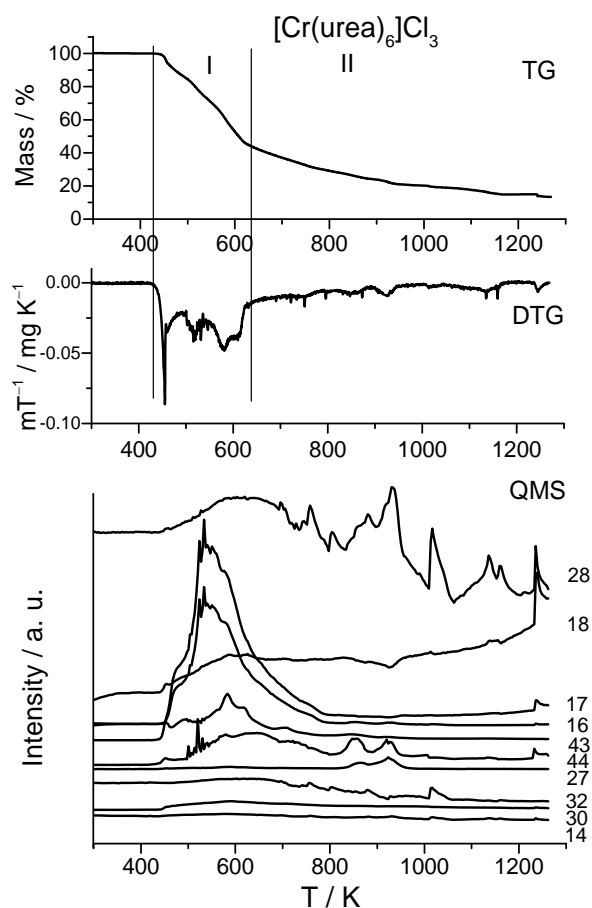
Figure 7. TG, DTG, and QMS curves obtained for [Cr(urea)$_6$]Cl$_3$ during heating with a constant rate of 10 Kmin^{-1}.

The TG-DSC analysis of [Cr(urea)$_6$]Cl$_3$ was already performed in the temperature range of 300–1070 K, in argon flow, at heating rate of 10 Kmin^{-1} by Qiu and Gao[34]. The compound is thermally stable up to 440 K. It decomposes in two main stages. In the first stage, between 440 and 620 K, the Cr–O coordination bonds break and disintegration of the urea molecules occurs with formation of solid CrCl$_3$·xNH$_3$. In the second stage, between 620 and 1070 K, most possibly the final solid (ClCrNH)$_n$ is created with releasing of volatile HCl and NH$_3$.

We reinvestigated the decomposition of [Cr(urea)$_6$]Cl$_3$ compound in the temperature range 300–1270 K using quadruple mass spectroscopy to analyze the gases evolved during TGA analysis. The TG, DTG, and QMS curves for [Cr(urea)$_6$]Cl$_3$ are shown in Fig. 7. The masses of m/e = 28, 18, 17, 16, 43, 44, 27, 32, 30, and 14 correspond to fragments of N$_2$, NH$_4$, NH$_3$, O or NH$_2$, HNCO, CO$_2$ or N$_2$O, HCN, O$_2$, NO, and N, respectively. The decomposition of the sample proceeds in two main stages. The TG curve shows that the composition is almost unchanged until 440 K. In the temperature range of 440–630 K it decomposes liberating and degrading the urea ligands and possibly creating an adduct such as CrCl$_3$·xNH$_3$. 45.0 % of the initial mass of the sample remains at 630 K what corresponds well to the CrCl$_3$·xNH$_3$ with x between 4 and 5. In the second stage, further degradation of urea molecules occurs together with constant releasing of chlorine. At 1270 K the thermal decomposition is not completely finished. 14.0 % of the

initial mass of the sample remains at this temperature and we assume that the solid remaining is the mixture of metallic Cr, CrCl$_3$ and ClCrNH.

Conclusions

Apart from elemental analysis the spectroscopic analysis of FT-IR and FT-RS spectra together with electronic spectra (UV-Vis) confirmed proper composition of the investigated compounds.

[Cr(urea)$_6$](BF$_4$)$_3$ crystallizes at 293 K in trigonal crystal system in space group *R*-3*c* with $a = b$ = 17.8250(5) Å, c = 13.9010(8) Å, and α, γ = 90°, β = 120°. Each Cr^{3+} cation is coordinated by six oxygen atoms deriving from urea molecules. The BF$_4^-$ anions are dynamically disordered. The compound is isostructural with [Cr(urea)$_6$](ClO$_4$)$_3$ and [Cr(urea)$_6$]Cl$_3$.

One solid-solid phase transition has been detected in [Cr(urea)$_6$](ClO$_4$)$_3$ at: T^h_C=298.4 K and in [Cr(urea)$_6$](BF$_4$)$_3$ at: T^h_C=255.4 K. Both transitions are characterized by very small thermal hysteresis (ca. 1-2 K) and are most probably of order-disorder type.

In argon atmosphere, [Cr(urea)$_6$](ClO$_4$)$_3$ decomposes explosively just above 500 K. [Cr(urea)$_6$](BF$_4$)$_3$ decomposes in the range of 470–1250 K in three main stages with Cr$_2$O$_3$ being a final product of decomposition. The thermal decomposition of [Cr(urea)$_6$]Cl$_3$ proceeds in two main stages. The product of decomposition, which is still not finished at 1270 K, is a mixture of Cr, CrCl$_3$ and ClCrNH.

Acknowledgements

References

[1]Li, J., Yang, X., Ishigaki, T., *J. Phys. Chem. B*, **2006**, *110*, 14611.

[2]Qiu, Y., Gao, L., *J. Am. Ceram. Soc.*, **2004**, *87*, 352.

[3]Qiu, Y., Gao, L., *Int. J. Inorg. Mater.*, **2004**, *19*, 63.

[4]Baker, J., Figgis, B. N., *Aust. J. Chem.*, **1980**, *33*, 2377.

[5]Yersin, H., Otto, H., Gliemann, G., *Theoret. Chim. Acta*, **1974**, *33*, 63.

[6]Davis, P. H., Wood, J. S., *Chem. Phys. Lett.*, **1969**, *4*, 466.

[7]Todorov, T., Petrova, R., Kossev, K., Macíček, J., Angelova, O., *Acta Cryst. C*, **1998**, *54*, 927.

[8]Figgis, B. N., Wadley, G. B., *J. Chem. Soc. Dalton Trans.*, **1972**, 2182.

[9]Aghabozorg, H., Stoufer, R. C., Hall, J. H., *Amirkabir (J. Science & Technology)*, **1987**, *2*, 28.

Eur. Chem. Bull., **2014**, *3(5)*, 474-481

480

[10]Mooy, J. H. M., de Jong, H. J., Glasbeek, M., van Voorst, J. D. W., *Chem. Phys. Lett.*, **1973**, *18*, 51.

[11]Mooy, J. H. M., Krieger, W., Heijdenrijk, D., Stam, C. H., *Chem. Phys. Lett.*, **1974**, *29*, 179.

[12]Mooy, J. H. M., Bolhuis, J., *Solid State Commun.*, **1976**, *19*, 1005.

[13]Aghabozorg, H., Palenik, G. J., Stoufer, R. C., Summers, J., *Inorg. Chem.*, **1982**, *21*, 3903.

[14]Figgis, B. N., Wadley, L. G. B., Graham, J., *Acta Crystallogr. B*, **1972**, *828*, 187.

[15]Figgis, B. N., Wadley, L. G. B., *Aust. J. Chem.*, **1972**, *25*, 2233.

[16]Górska, N., Inaba, A., Hirao, Y., Mikuli, E., Hołderna-Natkaniec, K., *RSC Adv.*, **2012**, *2*, 4283.

[17]Dołęga, D., Mikuli, E., Górska, N., Inaba, A., Hołderna-Natkaniec, K., Nitek, W., *J. Solid State Chem.*, **2013**, *204*, 233.

[18]Mikuli, E., Górska, N., Wróbel, S., Ściesiński, J., Ściesińska E., *Z. Naturforsch. A*, **2007**, *62a*, 179.

[19]Dołęga, D., Mikuli, E., Inaba, A., Górska, N., Hołderna-Natkaniec, K., Nitek, W., *J. Solid State Chem.*, **2013**, *197*, 429.

[20]Górska, N., Inaba, A., Hirao, Y., Mikuli, E., *J. Coord. Chem.*, **2013**, *66*, 1238.

[21]Mikuli, E., Górska, N., Wróbel, S., Ściesiński, J., Ściesińska E., *J. Mol. Struct.*, **2004**, *692*, 231.

[22]Mikuli, E., Migdał-Mikuli, A., Meyer, J., *J. Therm. Anal.*, **1998**, *54*, 93.

[23]Sinha, M. P., Pal, A., Dutta Roy, S. K., *J. Phys. C: Solid State Phys.*, **1976**, *9*, 2783.

[24]Szostak, E., Migdał-Mikuli, A., Hołderna-Natkaniec, K., Gwoździk-Bujakowski, R., Kaczor, A., *J. Coord. Chem.*, **2012**, *65*, 2732.

[25]Szostak, E., Migdał-Mikuli, A., *J. Therm. Anal. Cal.*, **2010**, *101*, 601.

[26]Werner, A., *Lieb. Ann. Chem.*, **1902,** *322*, 296.

[27]Keuleers, R., Desseyn, H. O., Rousseau, B., Van Alsenoy, C., *J. Phys. Chem.*, **1999**, *103*, 4621.

[28]Theophanides, T., *Coord. Chem. Rev.*, **1987**, *76*, 237.

[29]Penland, R. B., Mizushima, S., Curran, C., Quagliano, J. V., *J. Am. Chem. Soc.*, **1957**, *79*, 1575.

[30]Elving P. J., Zemel B., *J. Am. Chem. Soc.*,**1957**, *79*, 1281.

[31]Dingle, R., *J. Chem. Phys.*, **1969**, *50*, 1952.

[32]Witzke, H., *Theoret. Chim. Acta*, **1971**, *20*, 171.

[33]Górska, N., Inaba, A., Migdał-Mikuli, A., *Vib. Spectrosc.*, **2012**, *62*, 222.

[34] Qiu, Y., Gao L., *Matter. Res. Bull.*, **2003**, *38*, 1551.